

Phase identification of triphenylene-based discotic monomer and its main chain polymers

Tao Wang^a, Donghang Yan^{a,*}, Enle Zhou^a, Olaf Karthaus^b and Helmut Ringsdorf^b

^a*Polymer Physics Laboratory, Changchun Institute of Applied Chemistry, Chinese Academy of Sciences, Changchun 130022, People's Republic of China*

^b*Institute of Organic Chemistry, University of Mainz, J-J-Becher-Weg 18–20, D-55099 Mainz, Germany*

(Received 24 June 1997; revised 18 August 1997; accepted 25 August 1997)

A monomer, 2,3,6,7,10,11-hexakis(pentyloxy) triphenylene (HPT) possesses a triphenylene core as a discotic mesogen. Polymers containing this discotic mesogen have been studied using wide-angle X-ray and electron diffraction. HPT is known to show a discotic liquid crystal phase, noted as D_{ho} (h for hexagonal bidimensional lattice, o for ordered molecular spacing in each column). In this paper, however, HPT liquid crystalline phases, heated up from the crystalline state and cooled down from the isotropic state, were characterized in the diameter dimensions. In addition, the diameters of the columns are close to a parameter of two separate crystals. A core orientation was, therefore, proposed in the mesophase obtained by heating the crystalline. In order to distinguish these differences, the D_{ho} phase was divided to include the D_{hcd} and D_{hco} phases. Molecular modeling was performed to help our understanding of the orientation. The D_{hcd} and D_{hco} phases were used to characterize the phases of the discotic polymeric analogs by comparing their column diameters to those of the monomers. © 1998 Published by Elsevier Science Ltd. All rights reserved.

(Keywords: discotic liquid crystal; polymorphism; metastability)

INTRODUCTION

The synthesis and structural characterization of triphenylene-based discotic monomers and polymers have been widely investigated owing to their one-dimensional photo and electronic transition properties^{1,2}. The hexagonal symmetry of columns in the D_{ho} phase, generally formed by discotic hexa-*n*-alkoxy triphenylenes, has been elucidated by wide-angle X-ray diffraction (WAXD) and optical microscopy methods^{3,4}. Recent NMR studies revealed that the hexagonal symmetry of columns in the D_{ho} phase is due to the fast, free rotation of discs around their column axes^{5,6}. However, detailed electron diffraction intensity analysis indicates a pseudo-hexagonal symmetry in the columnar phase of the HPT system during heating of the crystalline state⁷. The same symmetrical character was also detected in the polymeric system.

Our previous work showed that lower symmetry in the hexagonal columnar phase results from the memory of core orientation in the crystalline state. The dimensions of the hexagonal lattice formed during heating is smaller than those of the lattice formed during cooling⁸. In this work, molecular modeling simulating the effects of free or restricted rotations of discs on the symmetry and packing behavior of columns is performed. This simulation allows better understanding of the nature of molecular packing in experimental lattice parameters and symmetry.

EXPERIMENTAL

Materials

The monomer sample used in this work (*Figure 1*), 2,3,6,7,10,11-hexakis(pentyloxy) triphenylene (HPT), was synthesized and subsequently purified as described as previously published⁹. The HPT crystal melted at 69°C and displayed a mesophase ranging from 69 to 10122°C. Polymer samples, abbreviated as MCDP10 and MCDP14, were main chain polymers containing HPTs with different spacers ($n = 10$ and 14)¹⁰. They showed mesophases ranging from 35 to 195°C for MCDP10 and 60 to 150°C for MCDP14, respectively.

Instruments

Thermal transitions were measured using a Perkin-Elmer DSC-2C at a heating rate of 10°C/min under nitrogen atmosphere. The optical textures of the sample were observed with a Zeiss–Carl Jena polarized light microscope with a hot stage. Wide-angle X-ray diagrams (Ni-filtered, Cu K α radiation, $\lambda = 0.154$ nm) were recorded in reflection mode with a Philips PW-1700 automated powder diffractometer. Electron diffraction patterns were obtained using a JEOL 2010 transmission electron microscope operated at 200 kV. Computer modeling was performed on an Indigo workstation. The Cerius² 2.0 software package produced by Molecular Simulation Inc. USA was used.

Molecular modeling route for the columnar phase

The basic idea of molecular modeling for the columnar phase was based upon the molecular mean field theory of discogens^{11,12}. A suitable conformation which possessed the

* To whom correspondence should be addressed

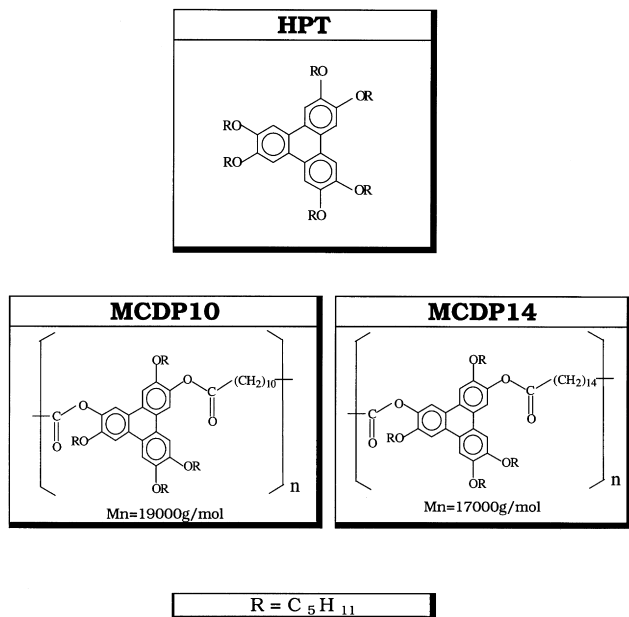


Figure 1 Molecular structure of discotic 2,3,6,7,10,11-hexakis(pentyl)oxy triphenylene (HPT) derivatives

highest spatial occupancy in the mesophase was chosen as an equivalent unit. The orientations of the unit were selected to be the free parameters in this calculation. Disogens oriented perpendicular to their columns were used as a limitation. The van der Waals surfaces of disogens were labeled with circles at the molecular outer contour. This was done to clearly show the arrangement of disogens in mutual orientations and the restrictions in rotation.

A triphenylene disogen with all *trans* side chains was first constructed in order to obtain a minimum energy conformation with the largest diameter of van der Waals contour. Conformation in the gas phase was then calculated by energy minimization under the Dreiding II force field¹³. The hexagonal lattice, which had been derived from diffraction experiments, and the minimized molecule were then chosen from the Crystal Builder and Crystal Packer modules incorporated in Cerius².

RESULTS AND DISCUSSION

The polymorphism of HPT

A diagram regarding the various HPT phases is shown in Figure 2. The CI and the CII are crystalline states, while the LCI and the LCII are mesophases. Reversible phase transitions between the CI and the LCI can occur via heating or cooling. Further heating causes the LCI phase to enter the isotropic state. When the sample is being cooled from the isotropic state, the LCII phase is formed. Cooling the sample at a slow rate leads to the CI phase at room temperature, while quenching the LCII phase results in the CII phase. The CII possesses an enlarged cell and can transform to the CI after a long annealing time. The LCII and the CII can be transformed from one to another by quenching or heating. But the LCI can only be obtained via heating of the sample from the CI state.

The crystalline structures of CI and CII have been studied by the electron crystallography approach. They possess an orthorhombic lattice with a P2₂2 space group. The cell dimensions of CI are $a = 3.67$ nm, $b = 2.79$ nm, $c = 0.49$ nm, and the cell dimensions of CII are $a = 3.86$ nm,

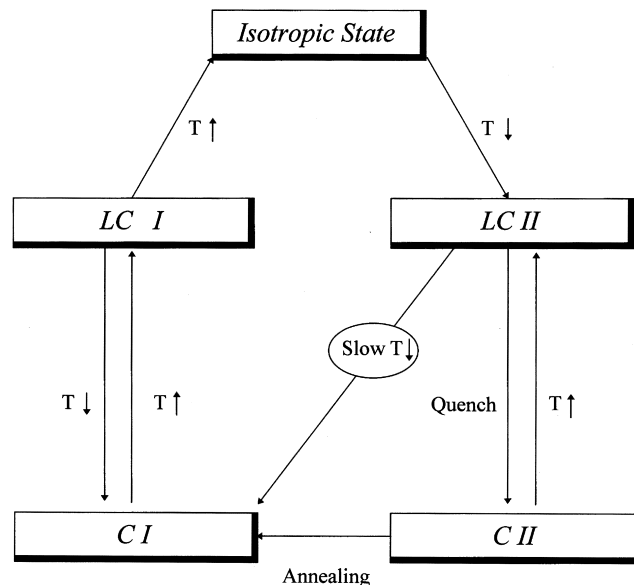


Figure 2 Polymorphism and phase transition of HPT. $T \uparrow$ refers to the ordinary speed of heating procedure, while $T \downarrow$ refers to the ordinary speed (lower than 20°C/min) of cooling procedure which is used for the quench process.

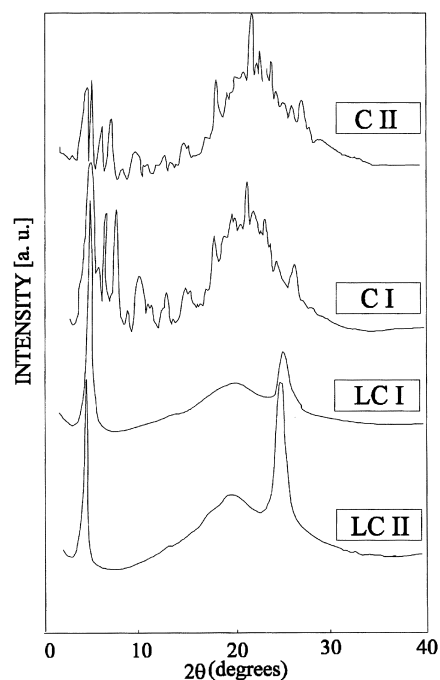


Figure 3 The WAXD patterns of HPT in crystalline and liquid crystalline states

$b = 2.91$ nm, $c = 0.50$ nm. Minimum packing energy calculations reveal that HPT molecules in these crystalline states are tilted about 48° with respect to the column axis. Columns form herringbone-like arrangements in the orthogonal two-dimensional lattice.

The WAXD diagrams of these phases are shown in Figure 3. The LCI mesophase possesses smaller hexagonal dimensions and is formed by heating the sample from the CI phase to 73°C. The LCII mesophase has larger hexagonal dimensions and is formed when the sample is cooled to 73°C from isotropic state. Cooling the LCII mesophase at a fast rate results in the CII crystalline phase with its correspondingly larger cell dimensions. In addition, cooling the sample

Table 1 Lattice constants of HPT in different phases

Phase	Lattice type	Cell constants
CI ^a	Orthorhombic	$a = 36.73 \text{ \AA}$, $b = 27.99 \text{ \AA}$, $c = 4.91 \text{ \AA}$
CII ^b	Orthorhombic	$a = 38.64 \text{ \AA}$, $b = 29.09 \text{ \AA}$, $c = 5.00 \text{ \AA}$
LCI ^c	Hexagonal	$a = 21.29 \text{ \AA}$, $c = 3.60 \text{ \AA}$
LCII ^d	Hexagonal	$a = 22.29 \text{ \AA}$, $c = 3.61 \text{ \AA}$

^aThe CI phase is the equilibrium melt-grown crystalline phase obtained by a slow temperature decreasing gradient from the isotropic state to room temperature

^bThe CII phase is obtained by quenching from the LCII mesophase

^cThe LCI phase is the mesophase obtained at 73°C by heating the CI phase from room temperature to 73°C

^dThe LCII phase is the mesophase obtained at 73°C by cooling the sample from the isotropic state

at a slow rate generates the CI phase. The detailed transformational thermal histories of these different phases (CI, CII, LCI and LCII) are given in Figure 2. The cell dimensions of various phases are summarized in Table 1. The existence of two liquid crystalline forms causes the D_{ho} phase to be divided into the D_{hed} (hexagonal bidimensional lattice with disordered core orientation) phase and the D_{hco} (hexagonal bidimensional lattice with ordered core orientation) phase in order to distinguish between the LCI and the LCII in the triphenylene system.

Amorphous halo from the flexible side chains can be observed in the WAXD diagrams of LCI and LCII. Most significantly, the diameter of the columns for the LCI is close to the dimension of the crystalline CI, and that of the LCII is close to that of the crystalline CII. A possible mechanism to form a core-oriented phase comes from the 'melting memory' of the core orientation in the crystalline phase, which is imposed by the space group symmetry. The core orientation phase in the LCI directly leads to a smaller hexagonal lattice in comparison with that of the core-non-oriented LCII phase.

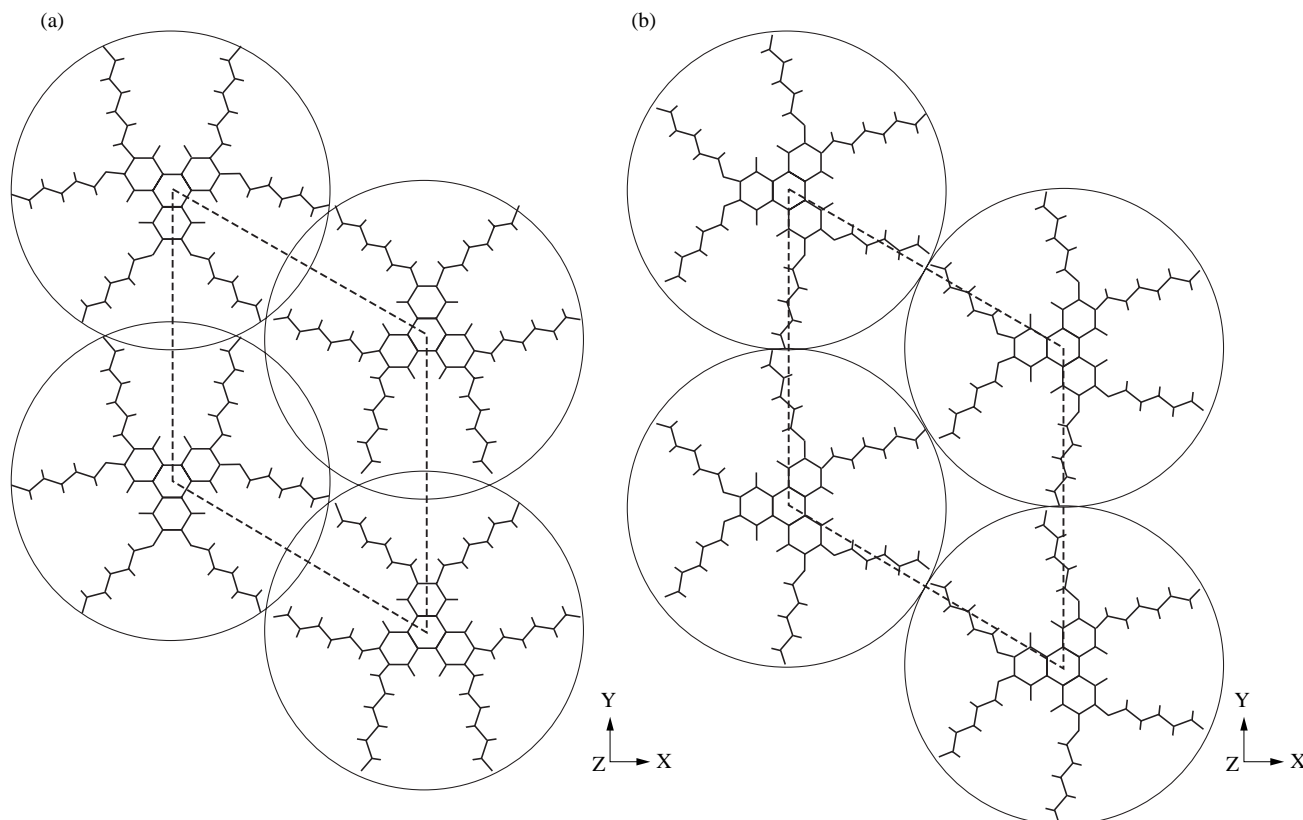
Thermal history and structure analysis indicates that the aggregation process of HPT is controlled by the crystallization of the aromatic cores. This behavior may be explained by a rigid planar core with flexible, or 'soft', edges in the liquid crystalline states. Due to these soft and hard components, experimental characterization of the aggregation kinetics is difficult.

The molecular modeling results of mesophases LCI and LCII are given in Figure 4. The van der Waals contour of the columns overlap in the LCI case, as shown in Figure 4a. The freedom of rotation is limited by this overlapping. The lower hexagonal symmetry of this phase was observed by electron diffraction intensity analysis⁷. In the case of LCII, the van der Waals contour of the columns does not overlap, as is shown in Figure 4b. This phase shows a higher ordered hexagonal symmetry which results from the fast, free rotation of discs along their columnar axis and was revealed by ²H NMR studies⁶.

The columnar phase structures of discotic polymers

In the monomer case, the high-density LCI phase is formed by heating the high-density CI phase. For this reason, the LCI phase keeps some of the packing order of the CI phase. Molecular modeling results reveal that the rotational freedoms of the HPT molecules are limited by the overlapping of their van der Waals contours. Core orientation is proposed to describe the packing character of the LCI phase. In the case of a main chain polymer, the length of the main chain spacer is a variable used to test the stability of the phases. Also, the rotational freedom of the discotic mesogen is restricted by a covalent linkage. Due to these differences, it is interesting to compare the packing characteristics of the polymer to that of the monomer.

The WAXD diagrams of the HPT monomer, and its corresponding polymers are given in Figure 5. MCDP10

**Figure 4** Molecular modeling results for LCI (a) and LCII (b) liquid crystalline phases viewed along the columnar axis

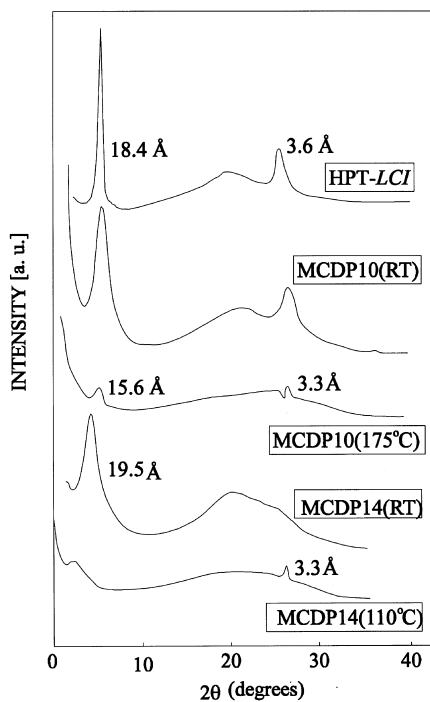


Figure 5 The comparison of WAXD diagrams of HPT, MCDP10 and MCDP14

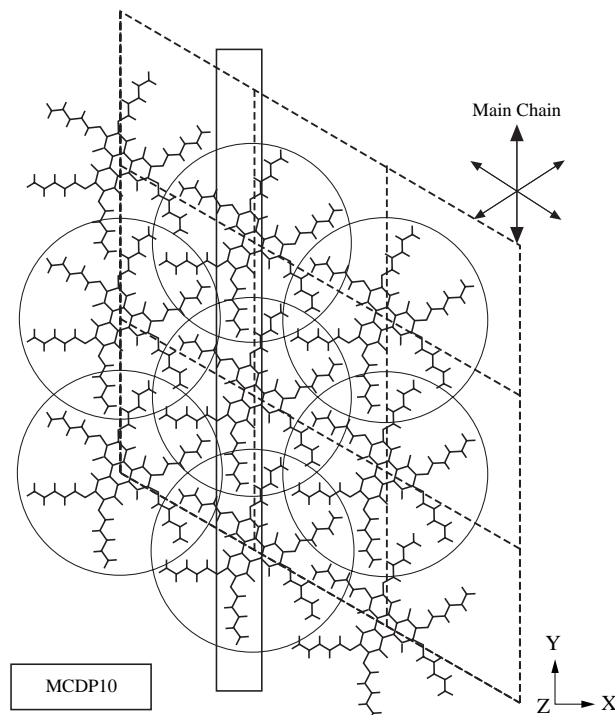


Figure 7 Schematic of disogens and main chain position in MCDP10's mesophase along the columnar axis

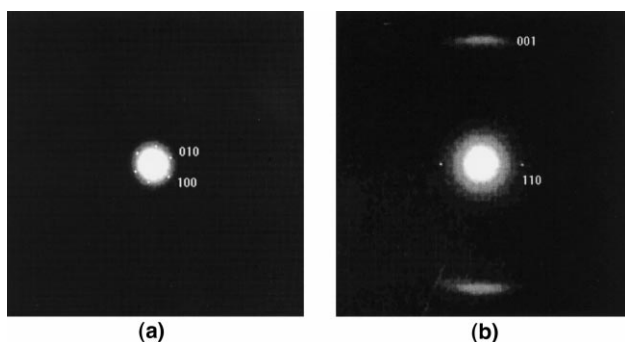


Figure 6 The electron diffraction patterns of MCDP10's columnar phase, (a) [001] zone and (b) [110] zone

and MCDP14 films were cast from a chloroform solution at room temperature. Both the inter- and intracolumnar regularities are observed. The MCDP10 has a smaller hexagonal packing dimension, while the MCDP14 has a larger hexagonal packing dimension at room temperature. When the MCDP10 sample is heated to 175°C, both the inter- and intracolumnar regular packings decrease. The lateral dimension of the hexagonal lattice, a , is 1.80 nm based on a (100) peak. In the case of MCDP14. At room temperature, the regularity of the intercolumnar packing is higher than that of the intracolumnar packing. When the sample is heated to 110°C, the regularity of the intracolumnar packing is higher than that of intercolumnar packing. The lateral dimension of the hexagonal lattice is 2.24 nm based on a (100) peak. This shows that regular stacking of the cores and hexagonal packing of the columns compete with each other. The hexagonal lattice constant a of MCDP14 is calculated as 2.24 nm.

Both MCDP10 and MCDP14 are in the liquid crystal state at room temperature. Therefore, the selected area electron diffraction patterns of the columnar phase can be obtained. *Figure 6a* can be indexed as the [001] zone, and *Figure 6b* is

the [110] zone. *Figure 6b* is most frequently observed, while *Figure 6a* is only occasionally found. These X-ray and electron diffractions indicate that these liquid crystal phases are in a hexagonal columnar packing. The columns in the upper and lower surface of the films exhibit dense packing and are favored to lie down in the plane of the sample film.

Molecular modeling results on the triphenylene disogen arrangement in the hexagonal lattice for MCDP10 are given in *Figure 7*. The main chains of the polymer are not directly given in the figure. But a possible position of the main chain is indicated with a rectangular shape. By geometric measurement, the alignment direction of the polymer main chain spacer among the disogens can be obtained (as shown in *Figure 8*). The length of the 10-carbon spacer in an all *trans* conformation was calculated as approximately 1.50 nm. The AD distance of 22.1 Å (*ca.*) is much longer than the length of a 10-carbon spacer. The only possible attachment of the main chain spacer is between columns which are nearest neighbors, such as AB, AC, and BC. The attachment of the main chain spacer between different layers of disogens is also allowed, since the column axis is perpendicular to the molecular plane. The mutual orientation of the disogens comes from the restriction of the linkage of the polymer main chain. The conformation characteristics of the main chain spacer can be inspected when the dynamic effects are ignored. Molecular mechanical calculations in the period lattice show that the main chain spacer may have a helical-like conformation which results from the unplanar configuration of carbonyl groups to the discotic cores (as shown in *Figure 9*).

For MCDP14, the structure exhibits hexagonal packing with a larger column diameter. This structure is probably controlled by the repulsion of the main chain spacer between disogens. This repulsion effect is observed in the WAXD at different temperature (*Figure 5*). Only the amorphous state can be obtained when the length of main chain spacer is increased to 20 carbons¹⁴.

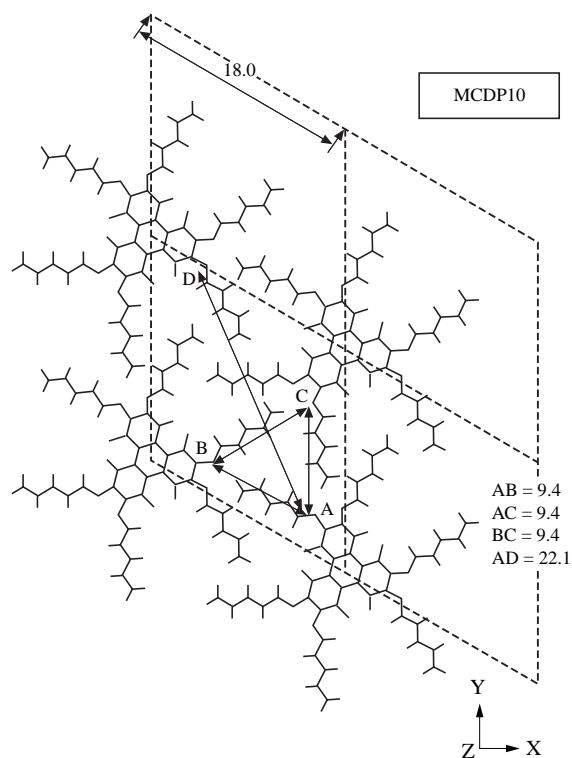


Figure 8 Geometric relationship of disogens in MCDP10's mesophase. The measurements indicated are in length units of Å

CONCLUSIONS

The D_{ho} phase is divided into the D_{hco} phase and the D_{hcd} phase. The core-oriented hexagonal columnar phase, D_{hco} , can be formed both in monomeric and polymeric triphenylene system, either by heating from the crystalline phase in the monomeric situation or from restriction of the polymer chain in the polymeric system. The core-oriented phase can be identified by a hexagonal lattice which is smaller than the large hexagonal lattice of the free rotation mode. Molecular modeling shows that the rotation of molecules along the axis of the column is free in the larger hexagonal lattice, while the rotation is restricted in the smaller hexagonal lattice.

ACKNOWLEDGEMENTS

The authors gratefully acknowledge financial support from the National Key Projects for Fundamental Research 'Macromolecular Condensed State', the State Science and Technology Commission of China. The author also grate-

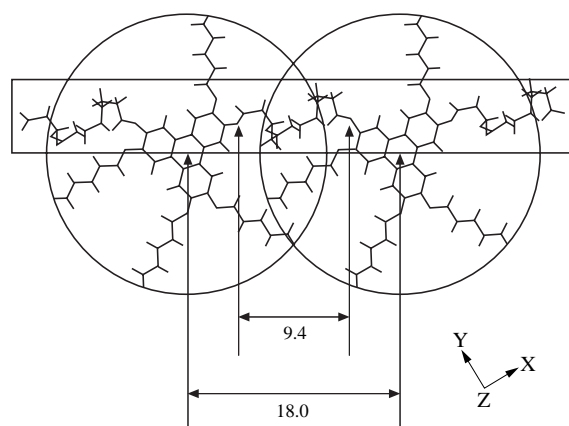


Figure 9 Calculated main chain spacer conformation of MCDP10 when overlooking the dynamic effect; length unit, Å

fully acknowledges the support of the K. C. Wong Education Foundation in Hong Kong.

REFERENCES

1. Adam, D., Closs, F., Frey, T., Funhoff, D., Haarer, D., Ringsdorf, H., Schuhmacher, P. and Siemensmeyer, K., *Phys. Rev. Lett.*, 1993, **70**, 457.
2. Boden, N., Bushby, R.J. and Clements, J., *J. Chem. Phys.*, 1993, **98**, 5920.
3. Billard, J., in: *Liquid Crystals of One and Two Dimensional Order*, Vol. 11, ed. W. Helfrich and G. Heppke. Springer Verlag, Berlin, 1980.
4. Chandrasekhar, S., in: *Advances in Liquid Crystals*, Vol. 5, ed. G. H. Brown. Academic Press, New York, 1982.
5. Kranig, W., Boeffet, C., Spiess, H.W., Karthaus, O., Ringsdorf, H. and Wustefeld, R., *Liquid Crystals*, 1990, **8**(3), 375.
6. Kranig, W., Boeffet, C. and Spiess, H.W., *Macromolecules*, 1990, **23**, 4061.
7. Voigt-Martin, I.G., Garbella, R.W. and Schumacher, M., *Macromolecules*, 1992, **25**, 961.
8. Wang, T., Yan, D., Zhou, E., Karthaus, O. and Ringsdorf, H., submitted to *Liquid Crystals*.
9. Kreuder, W. and Ringsdorf, H., *Makromol. Chem., Rapid Commun.*, 1983, **4**, 807.
10. Kreuder, W., Ringsdorf, H. and Tschirner, P., *Makromol. Chem., Rapid Commun.*, 1985, **6**, 367.
11. Chandrasekhar, S., Savithramma, K. L. and Madhusudana, N. V., in: *Liquid Crystals and Ordered Fluids*, Vol. 4, ed. A. C. Giffin and J. F. Johnson. Plenum, New York, 1984, p. 299.
12. Ghose, D., Bose, T.R., Mukherjee, C.D., Roy, M.K. and Saha, M., *Mol. Cryst. Liq. Cryst.*, 1989, **173**, 17.
13. Mayo, S.L., Olafson, B.D. and Goddard, W.A. III, *J. Phys. Chem.*, 1990, **94**, 8897.
14. Ringsdorf, H., Wustefeld, R., Zerta, E., Ebert, M. and Wendorf, J.H., *Angew. Chem. Int. Ed. Engl.*, 1989, **28**, 914.